

Supplemental Data

***miR-125a-5p* Regulates Megakaryocyte Proplatelet Formation Via the Actin Bundling Protein L-Plastin. Bhatlekar S et al.,**

Supplemental Methods

Human subjects

Donor recruitment, platelet isolation, RNA profiling on 154 healthy donors in the Platelet RNA And eXpression study 1 (PRAX1) have been previously described.^{1,2} This data set included platelet count, white blood cell count and hemoglobin, but not red blood cell count.

RNA profiling of primary human BM MKs, platelets and cultured MKs

Bone marrow (BM) aspirates and peripheral blood were obtained during the same encounter from two healthy donors. BM megakaryocytes (MKs) were identified by a Board-Certified Hematologist using standard morphologic criteria, and ~ 200 MKs were micro-dissected by laser capture scanning microscopy³ at the pathology core lab of Children's Hospital of Philadelphia (Philadelphia, Pennsylvania). Leukocyte and erythrocyte-depleted platelets were obtained as before.⁴ CD34+ cells were isolated from human umbilical vein cord blood, cultured in TPO as previously described⁵ (supplemental Figure 1), and CD61 purified MKs isolated on days 6, 9 and 13 using immunomagnetic beads. RNA was extracted using the Total RNA Purification kit (Norgen Bioteck, Inc. Ontario). 372 common miRs were quantified using miRCURY LNA Universal RT microRNA PCR Human Panel I (Exiqon, Inc. Vedbaek, Denmark). mRNAs were quantified by paired end run Hiseq2500 RNAseq (Illumina, San Diego, CA) at the Center for Applied Genomics, Children's Hospital of Philadelphia (Philadelphia, PA).⁵

miRCURY LNA microRNA PCR profiling and data analysis

miRCURY LNA Universal RT microRNA PCR Human Panel I was used (Exiqon, Inc. Vedbaek, Denmark). 30 ng RNA was reverse transcribed in 30 µl reactions using the miRCURY LNA™ Universal RT microRNA PCR, Polyadenylation and cDNA synthesis kit (Exiqon). cDNA was diluted 100x and assayed in 10 µl PCR reactions according to the protocol for miRCURY LNA™ Universal RT microRNA PCR; each microRNA was assayed once by qPCR on the microRNA Ready-to-Use PCR, Human panel I using ExiLENT SYBR® Green master mix. Negative controls excluding template from the reverse transcription reaction was performed and profiled like the samples. The amplification was performed in a LightCycler® (LC) 480 Real-Time PCR System (Roche) in 384 well plates. The amplification curves were analyzed using the Roche LC software, both for determination of Cq (quantification cycle) (by the 2nd derivative method) and for melting curve analysis. For quality control, each RNA sample was successfully reverse transcribed (RT) into cDNA and tested for the expression of 5 miRNAs and one synthetic spike-in RNAs. All five microRNAs were detected in all samples. The expression level is very similar in all the samples, and comparable to other samples of this type. Furthermore, no RT-qPCR inhibition as judged by the expression of the included UniSp6 spike-in. The amplification efficiency was calculated using algorithms similar to the LinReg software. All assays were inspected for distinct melting curves and the Tm was checked to be within known specifications for the assay.

Furthermore, assays must be detected with 5 Cqs less than the negative control, and with Cq<37 to be included in the data analysis. Data that did not pass these criteria were omitted from any further analysis. Cq was calculated as the 2nd derivative. Using NormFinder

the best normalizer was found to be the average of assays detected in all samples. All data was normalized to the average of assays detected in all samples (dCq = average – assay Cq). Higher dCq value means higher expression and vice-versa.

RNA Sequencing

RNA sequencing was performed using Hiseq2500 (Illumina), a Paired End run, 2x125 cycles, in High Output. cDNA synthesis was performed using the Ovation® RNA-Seq System V2 (NuGEN Technologies, Inc. San Carlos, CA). The amplified cDNA was used for library preparation using the Ovation Ultralow System V2 (NuGEN Technologies). Alignments were generated using the ultrafast universal RNA-Seq aligner (STAR). Differential expression tests were performed using the cuffdiff package in cufflink 2.2.1 and the GTF file from GENCODE version 19, using only non-ribosomal RNA alignment reads.

Expression of a gene was represented as fragments per kilobase of transcript per million mapped reads (FPKM). mRNA transcripts with $FPKM > 0$ in all samples were only considered for all analysis.

Locked nucleic acid (LNA) inhibition and flow cytometry

miRCURY locked nucleic acid (LNA) inhibitors against *miR-125a-5p* or negative control A, referred as miR-125a LNA or negC LNA respectively (Exiqon Inc.) (100 nM) were added to day 3, 6 and 9 cultured MKs⁶ (supplemental Figure 1). For hematopoietic stem cells (HSC), hematopoietic stem and progenitor cells (HSPC) and MK marker assessment on *miR-125a-5p* inhibition, cultured cells at days 0 (without LNAs) and at days 3, 6, 9 and 13 (in presence of miR-125a or negC LNA control) stained with Brilliant Violet 510 anti-lineage (Lin) antibody (BioLegend, San Diego, CA), PE-Cy7 labeled anti-CD38, APC labeled anti-CD41a, PE labeled anti-CD42a (BDBiosciences, San Jose, CA) as described previously.⁵

Lentiviral transduction in cultured MKs

CD34+ hematopoietic stem cells (HSCs) and hematopoietic stem and progenitor cells (HSPCs) were isolated from human umbilical cord blood.⁵ *miR-125a-5p* and *LCP1* overexpression in cultured MKs was performed by lentiviral transduction as described (Supplemental figure 1).^{5,6} The human miR-125a-5p stem loop structure or coding sequence *LCP1* was cloned into pCDH-MSCV-GFP lentiviral vector at NheI and NotI sites by polymerase chain reaction (PCR) based strategy using platelet cDNA as template. All constructs were verified by DNA sequencing. Lentiviral constructs overexpressing miR-125a-5p or *LCP1* were co-transfected with the packaging vector pCMV8.74 and the envelope vector pMD2G (System Biosciences, Palo Alto, CA) into the HEK 293Ta cell line (GeneCopeia, Rockville, MD) using Lipofectamine 2000 (Invitrogen, Carlsbad, CA). Purified lentiviral particles were transduced (MOI of 5) in CD34+ cultures at day 3. Only transduced cultures with > 80% transduction efficiency on day 6 were cultured further and used for various assays. The transduced cells were cultured in serum free expansion media for 13 days as described before.⁵ For PPF assay, only GFP+ MKs were counted.

In vivo miR-125a-5p LNA studies

miR-125a-5p ('125a') LNA and negative control ('negC') LNA administered mice (n=8) were euthanized on day 10 using CO₂ asphyxiation. Blood was collected by cardiac puncture. RNA from leukocyte-, erythrocyte-, depleted platelets and bone marrow cells were isolated using Trizol method (Thermo Fisher Scientific, Waltham, MA). Murine *miR-125a-5p* levels in purified platelets and bone marrow cell were assessed by real time PCR. Spleen and liver organs were harvested from these mice for histopathology studies.⁷ The morphology of MKs in

bone marrow, spleen and liver was assessed by a board-certified pathologist (Dr. Allie Grossman). Femurs were collected from mice injected with *in vivo miR-125a* or nc LNA (n=4 each group and sectioned as previously described.^{8,9} MKs were stained using anti-VWF antibody (Dako, Carpinteria, CA)⁷, and VWF+ MKs per unit area were scored blinded for numbers. Staining procedure were done at the ARUP laboratories (Salt Lake City, Utah) and images were taken by axioscan slide scanner at cell imaging core facility of University of Utah (Salt Lake City, Utah).

CRISPR/Cas9 knock-down of L-plastin in MKs

Alt-R CRISPR/Cas9 gene editing was performed for L-plastin knock-down ('K-d') in cultured MKs. The protocol is modified from IDTDNA user method (Integrated DNA technologies, Inc. Newark, NJ). Alt-R CRISPR/Cas9 human LCP1 guide RNA (termed as '*LCP1* crRNA'), Alt-R tracrRNA and Alt-R electroporation enhancer (Integrated DNA technologies, Newark, NJ) were resuspended in RNase free 10 mM Tris buffer (pH 7.5). 12.5 μ M *LCP1* guide RNA and 5 μ M tracrRNA were added together in RNase free PCR tube and heated at 95°C for 5 minutes in thermal cycler with heated lid. This mixture (*LCP1* crRNA/tracrRNA) was incubated further for 10 minutes at room temperature. Next, ribonucleoprotein (RNP) complex consisting of 120 pmol of *LCP1* crRNA/tracrRNA and 105 pmol of Alt R spCas9 nuclease V3 (Integrated DNA technologies, Newark, NJ) were added together. Sterile RNase free 1x phosphate saline buffer (PBS) was added to the final volume of 5 μ L. This RNP complex was heated at 37 °C for 4 minutes in thermal cycler with heated lid. Next, 1×10^6 (per condition) human umbilical cord blood derived CD34+ cells at day 3 were harvested, washed with 1x PBS and resuspended in 20 μ L Amexa nucleofection solution P3 (set at room temperature) (Lonza, Basel, Switzerland). These cells were then added with RNP complex (described before) and 3.85 μ M Alt-R electroporation enhancer, transfected by nucleofection using P3 primary cell 4D-nucleofector X Kit S (Integrated DNA technologies, Newark, NJ) and Amexa 4D device (Lonza, Basel, Switzerland). Transfected cells were then plated into the 48 well plate for 48 hours and then transferred to the 24 well plate. Cells were cultured in serum free expansion media with cytokines as described before for 13 days.

LNA GapmeR inhibition of LCP1 in cultured MKs

For *LCP1* inhibition, LNA GapmeR against *LCP1* mRNA were synthesized (Exiqon Inc., Vedbaek, Denmark).¹⁰ Sequence of *LCP1* LNA GapmeR: GGTAATAAGCTTTTGA. Cultured cells were incubated with 500 nM *LCP1* LNA GapmeR or negative control A LNA GapmeR (referred as L-p GapmeR and negC GapmeR respectively) at days 3, 6 and 9. Day 13 MKs were harvested to assess *LCP1* mRNA by qPCR.

Migration assay

Migration of day 13 MKs was assessed in transwell migration assays using 8 μ m pore inserts¹¹, with stromal cell derived factor 1 alpha (SDF-1 α) in the lower chamber. After 2 hours, CD41a+/CD42a+ cells in lower chamber were counted by flow cytometry. Controls for normalization lacked SDF-1 α .

Transmission electron microscopy

Day 13 MKs were washed, pelleted and fixed for transmission electron microscopy (TEM) as before⁵, and imaged in a JEM-100CX II transmission electron microscope (JEOL Ltd., Tokyo).¹² At least 15 MKs per conditions were analyzed for IMS analysis.

Real time PCR

RNA was harvested using Trizol method (Life Technologies, Carlsbad, CA) and cDNA synthesis was prepared using manufacturer's instruction (Invitrogen, Carlsbad, CA). Taqman assays (Life Technologies, Carlsbad, CA) that measure only mature miR sequence by real time PCR were used to verify inhibition or overexpression of MK *miR-12a-5p*. *miR-30c-5p* was used as a normalizer as we have shown previously *miR-30c-5p* was determined to be an appropriate reference normalized for cross-cell real time PCR comparisons.¹³ *LCP1* mRNA levels were quantified by SYBR green (Thermo Fisher Scientific, Waltham, MA). Primers used were: *LCP1* forward: GTTGCCAAGACCTTTAGAAAAGC, *LCP1* reverse: GCCAACGCTAGACTGCTCT, *Lcp1* forward: TGTGCCAGACACGATTGACG, *Lcp1* reverse: TCGGCCCTATATTAACCACG, *ACTB* forward: ACCAACTGGGACGACATGGAGAAA, *ACTB* reverse: TTAATGTCACGCACGATTTCCCGC. *ACTB* was used as a normalizer. Relative mean fold changes were calculated according to the $2^{(-\Delta\Delta Ct)}$ method.

Immunofluorescence staining

Cultured MKs were stained as described previously.⁵ Briefly, day 13 MKs (with different experimental conditions) were plated at a density of 2.5×10^5 per 250 μ l cells/ml on immobilized human fibrinogen (100 μ g/ml; Calbiochem-Novabiochem Corporation, San Diego, CA) in a single well of 8-well chamber slide using a fresh serum free stem cell expansion medium supplemented with 50 ng/mL TPO. Cells were cultured in 37°C, 5% CO₂ incubator overnight. Cells were fixed with 4% paraformaldehyde. For co-localization studies, MKs were stained with anti-LCP1 antibody (LifeSpan Biosciences, Inc., Seattle, WA) and filamentous actin (F actin) (ActinRed 555 ReadyProbes, Thermo Fisher Scientific, Waltham, MA). Alexa fluor 488 (Thermo Fisher Scientific, Waltham, MA) was used as secondary antibody. Cells were stained with a nuclear stain, DAPI (Molecular Probes, Eugene, OR) for 10 minutes at room temperature. Proplatelets were stained using anti- α tubulin antibody (cell signaling, Danvers, MA) as described.⁵ For podosomes staining, MKs were stained with alexa fluor 488 WASP antibody (B-9, Santa Cruz Biotechnology, Inc., Dallas, TX) and F actin (ActinRed 555 ReadyProbes, Thermo Fisher Scientific, Waltham, MA).

Western blotting

Day 13 or 11 cultured MKs were lysed using lysis buffer (Cell signaling technology, Danvers, MA) and proteins were separated by SDS-page.⁵ L-plastin protein was probed using anti-LCP1 antibody (LifeSpan Biosciences, Inc., Seattle, WA). Anti-actin or anti-GAPDH (Santa Cruz Biotechnology, Inc., Dallas, TX) was used as a control for protein loading and densitometric quantification. Densitometric quantification was done by LI-COR (LI-COR Biosciences Lincoln, NE).

Reporter gene activity assays

HEK293T were transfected with the psiCHECK-2 vector (Promega, Madison, WI) containing either the wildtype or mutated (10 nucleotides at predicted binding sites were mutated) 3' untranslated region (UTR) of L-plastin located downstream of Renilla coding region in conjunction with Pre-miR miRNA Precursor of *miR-125a-5p* (mimic) or a non-targeting miR negative control ('ntc') (Thermo Fisher Scientific, Waltham, MA). Values were corrected for transfection efficiency and subsequently represented as luminescence output generated by the pre-*miR-125a-5p* mimic normalized to output from ntc.

Argonaute 2 Immunoprecipitation

Argonaute 2 (Ago2) immunoprecipitation was performed as previously described.⁶

Total internal reflection fluorescence microscopy (TIRF)

Day 10 MKs were immobilized on human fibrinogen (100 µg/ml; Calbiochem-Novabiochem Corporation, San Diego, CA) in medium overnight with 50 ng/mL TPO for 12 hours, fixed with 4% paraformaldehyde, stained for filamentous actin (F actin) (ActinRed 555 ReadyProbes, Thermo Fisher Scientific, Waltham, MA) and imaged using an ELYRA inverted microscope with a 100X objective, 1.46 numerical aperture (Zeiss, Oberkochen, Germany). The 568 nm laser was set with the angle of the laser to achieve TIRF (with a penetration depth of 100 nm).¹⁴

Image analysis

MK staining and structures were quantified blinded to the treatment: (1) VWF staining by Fiji version software;¹⁵ podosomes by ImageJ (National Institute of Health, Bethesda, Maryland)¹⁶; IMS by binary editor function of NIS element software (Nikon, Minato, Tokyo, Japan).

Bioinformatics analysis

Putative mRNA targets of *miRNA-125a-5p* were predicted by miRwalk 2.0 (<http://www.umm.uni-heidelberg.de/apps/zmf/mirwalk/>)^{17 18} and sequences were aligned using RNA hybrid (<http://bibiserv.techfak.uni-bielefeld.de/rmahybrid/>). Heat maps were generated using metaboanalyst software (<https://www.metaboanalyst.ca/faces/Secure/upload/StatUploadView.xhtml>).

Statistical analysis

Spearman rank correlation (ρ) was calculated for miRNAs. Pearson correlation (R) was calculated for *miR-125a-5p* expression levels with platelet count, white blood cells, hemoglobin or *LCP1* expression levels with platelet count. All other statistical analyses were performed using GraphPad Prism 6 software version 10.1 (La Jolla, CA) and reported as mean \pm standard error of mean (SEM). All 'n' presented in this manuscript represents biologic and separate donors, cord bloods or mice. Fold changes for *miR-125a-5p* levels and L-plastin *in vitro* and *in vivo* were compared to their respective controls and significance determined by one sample t test. For *in vivo miR-125a-5p* LNA inhibition, one tailed Mann Whitney U test was used for calculating statistical significance. For all other analyses, statistical significance was assessed using 2-tailed paired student's t test. $P < 0.05$ was considered significant.

Supplemental Tables (attached separately)

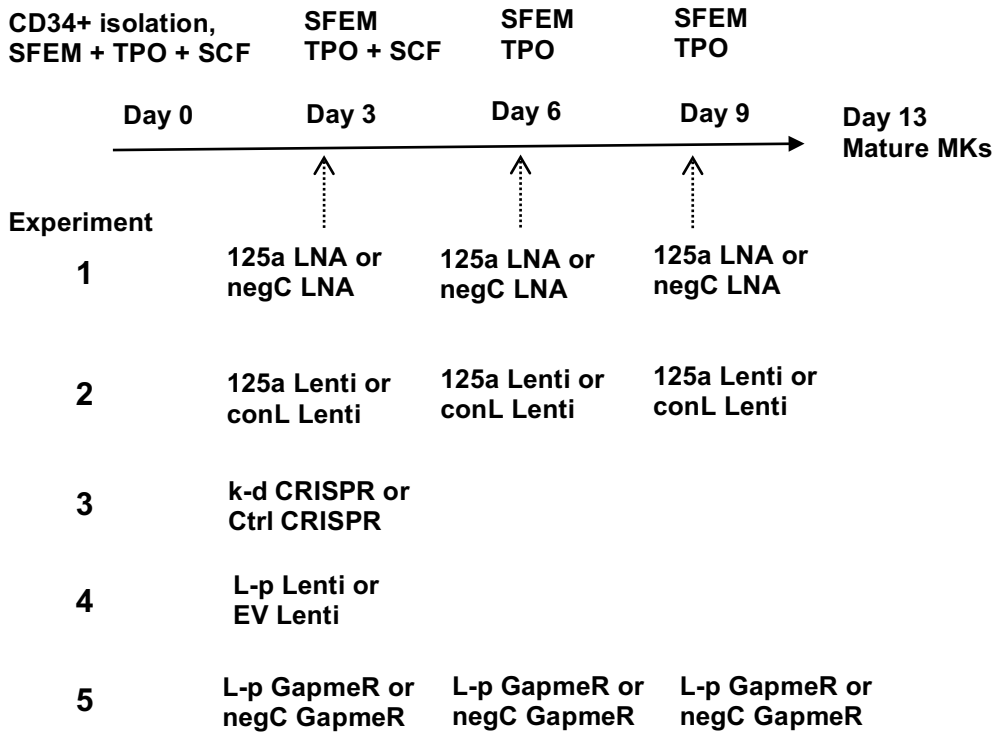
Supplemental Table 1. List of miRs expressed in BM MKs and platelets isolated from the same healthy donors.

Supplemental Table 2. Comparison of relative miR expression between primary, mature human BM MKs and cord blood-derived day 13 (D13) cultured MKs.

Supplemental Table 3. Platelet miRs associated with peripheral blood platelet count.

Supplemental Table 4. Changes in mRNA levels in differentiating human CD61+ cultured MKs.

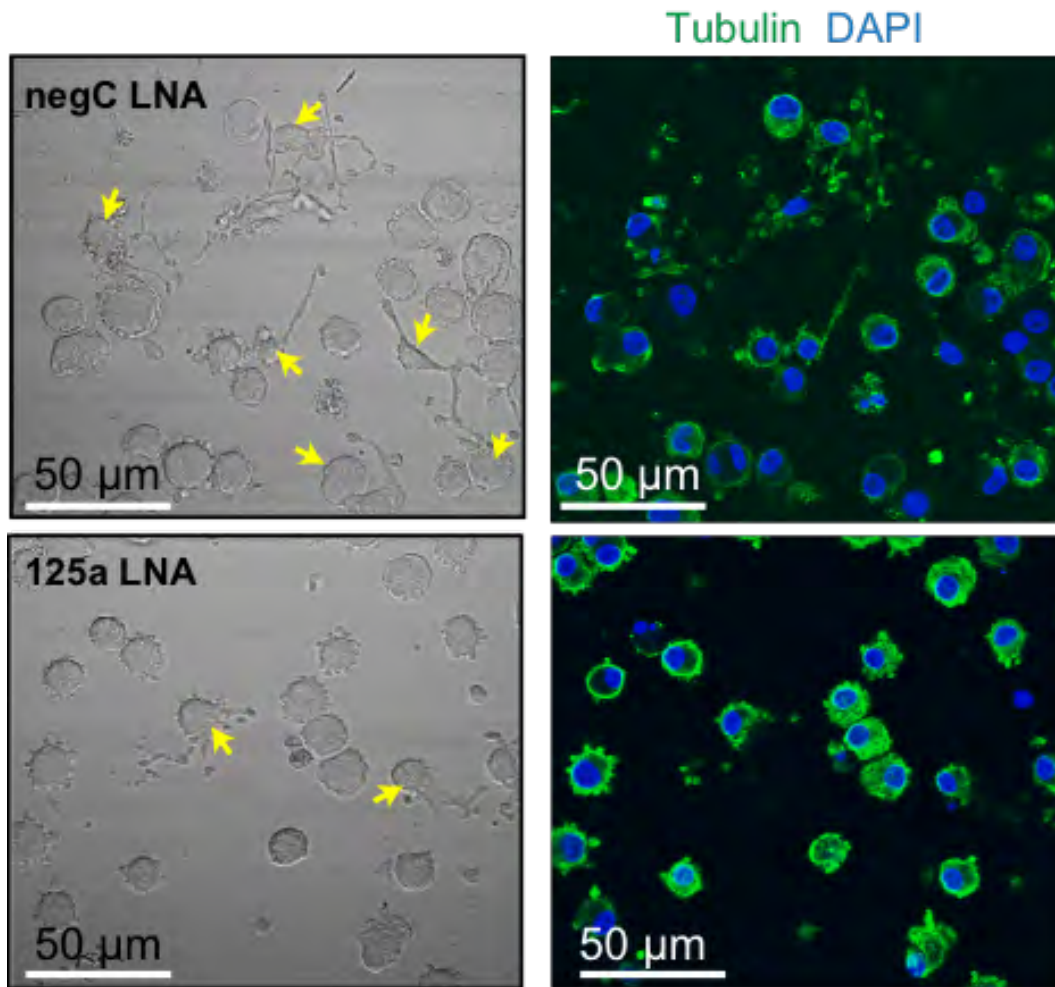
Supplemental Figures



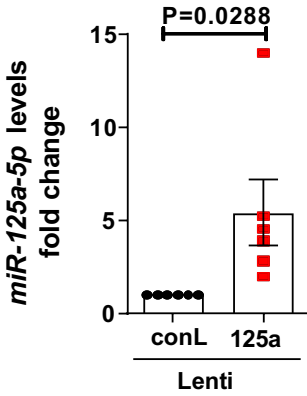
Supplemental Figure 1. Culturing and experimental conditions. On day 0, CD34+ cells were isolated from human umbilical cord blood using immunomagnetic beads and cultured at 1×10^6 cells/mL in serum free expansion media (SFEM) with 25 ng/ml stem cell factor (SCF) and 20 ng/ml thrombopoietin (TPO). Media was changed on days 3, 6 and 9; days 6 and 9 had no SCF and TPO was increased to 50 ng/mL.

Experimental conditions.

1. Locked nucleic acid (LNA) inhibition. 100 nM *miR-125a-5p* (125a LNA) or negative control (negC LNA) was added on days 3, 6 and 9.
2. Lentiviral overexpression (OE). Day 3 cells were transduced with lentivirus with *miR-125a-5p* (125a Lenti) or negative lentiviral control (conL).
3. L-plastin CRISPER/Cas9 knockdown. Day 3 cells were transfected by nucleofection with L-plastin CRISPR RNA (k-d CRISPR) or scrambled control (ctrl CRISPR).
4. Lentiviral overexpression (OE). Day 3 cells were transduced with lentivirus with L-plastin (L-p Lenti) or empty lentiviral plasmid (EV Lenti) negative control.
5. L-plastin GapmeR LNA inhibition. 500 nM *LCP1* (L-p GapmeR) or negative control (negC gapmeR) was added on days 3, 6 and 9.

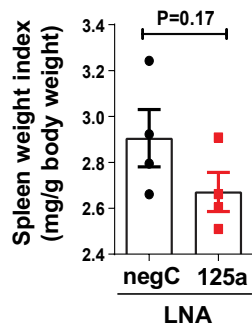


Supplemental Figure 2. *miR-125a-5p* regulates proplatelet formation (PPF) in cultured MKs. Representative brightfield (left) images of MKs with proplatelets (PPs) (yellow arrows) on *miR-125a-5p* inhibition. Tubulin stained PP (green) are shown (right) for the same objective field, as brightfield images. Blue color indicates a nuclear stain, DAPI.

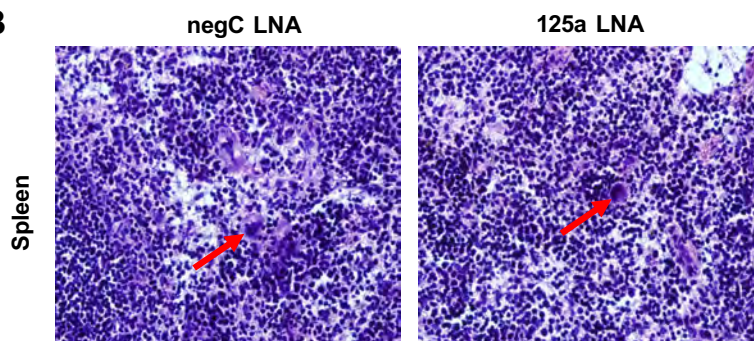


Supplemental Figure 3. *miR-125a-5p* overexpression in cultured MKs by lentiviral transduction. Day 3 cells were transduced with negative control lentiviral control (conL) or *miR-125a-5p* lentiviral particles (125a Lenti). Transduced cells were cultured for 13 days in MK favoring culture conditions. RNA from day 13 MKs were harvested and *miR-125a-5p* levels were assessed by real time PCR. Fold changes of *miR-125a-5p* overexpression on lentiviral transduction was plotted for conL vs. 125a lenti, normalized to *miR-30c* levels (n=6).

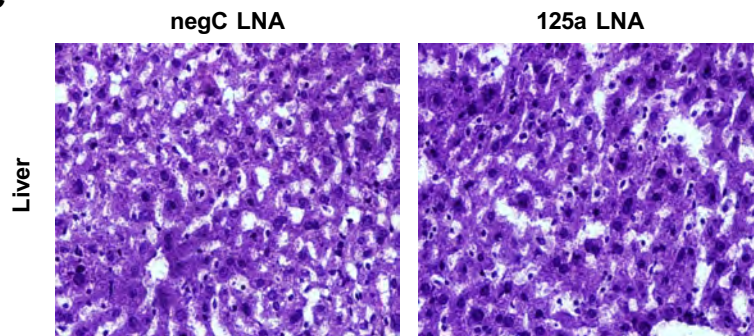
A



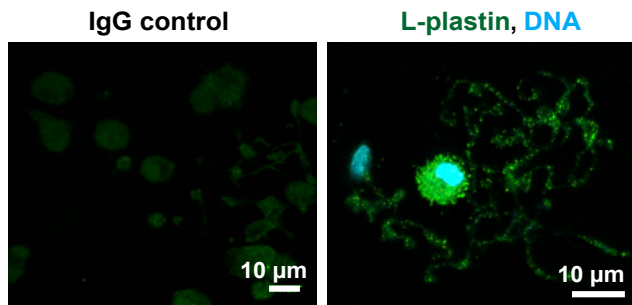
B



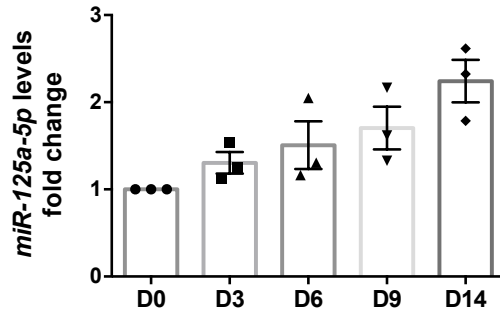
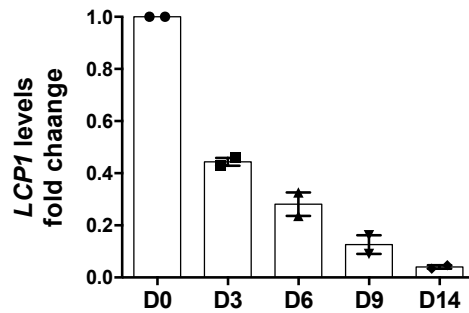
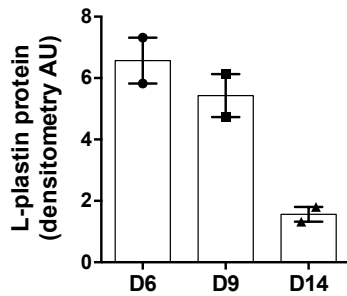
C



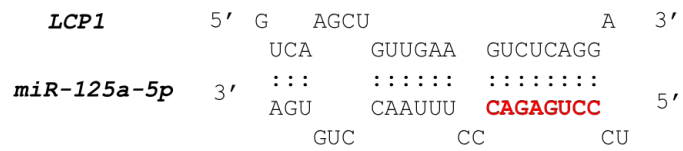
Supplemental Figure 4. Mouse spleen and liver histology after *in vivo* inhibition of *miR-125a-5p*. **A.** Spleen weight index measured as spleen weight (in milligrams, mg) over total body weight (in grams, g) for mice injected with negative control LNA (negC LNA) or *miR-125a-5p* LNA (125a LNA) (n=4). **B-C.** Representative images of hematoxylin and eosin (H&E) staining of murine **(B)** spleen and **(C)** liver injected with negC or 125a LNAs. In panel (B) red arrow indicates MK.



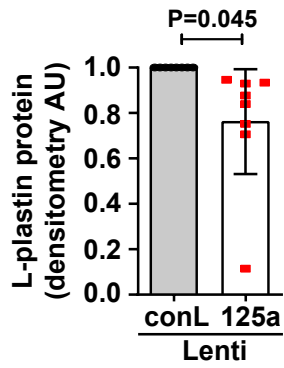
Supplemental Figure 5. IgG control for L-plastin immunofluorescence staining in cultured MKs. Representative images of day 14 MKs with or without proplatelets. IgG control (left) and L-plastin staining in green (right) is shown. Scale bar=10 μ m.

A**B****C**

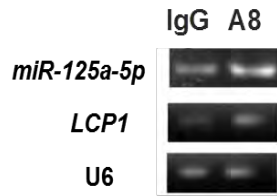
Supplemental Figure 6: *miR-125a-5p* and L-plastin expression changes during MK differentiation in cultures. **A.** *miR-125a-5p* levels quantified by qRT-PCR in CD34+ cord blood derived MK cultures at days 0, 3, 6, 9 and 14. *miR-30c* used for normalizer (n=3 independent cultures, P=0.036 d0 vs. d14). **B.** *LCP1* mRNA levels quantified by qRT-PCR in CD34+ cord blood derived MK cultures at days 0, 3, 6, 9 and 14 (n=2 independent cultures). **C.** Densitometric quantification of L-plastin immunoblot for days 6, 9 and 14 (n=2 independent cultures). GAPDH used as normalizer for quantification.



Supplemental Figure 7. *miR-125a-5p* predicted to target 3' untranslated region (UTR) of *LCP1*. A. *miR-125a-5p* predicted to target 3' untranslated region (UTR) of *LCP1*. The nucleotide sequence information of *miR-125a-5p* and its target site in 3' UTR of *LCP1*. Red color indicates *miR-125a-5p* seed sequence. Dotted lines denote nucleotide base pairing of *miR-125a-5p* and *LCP1*. Binding site in *LCP1* mRNA has a strong affinity to the *miR-125a-5p* (free energy = -24.1 kcal/mol).



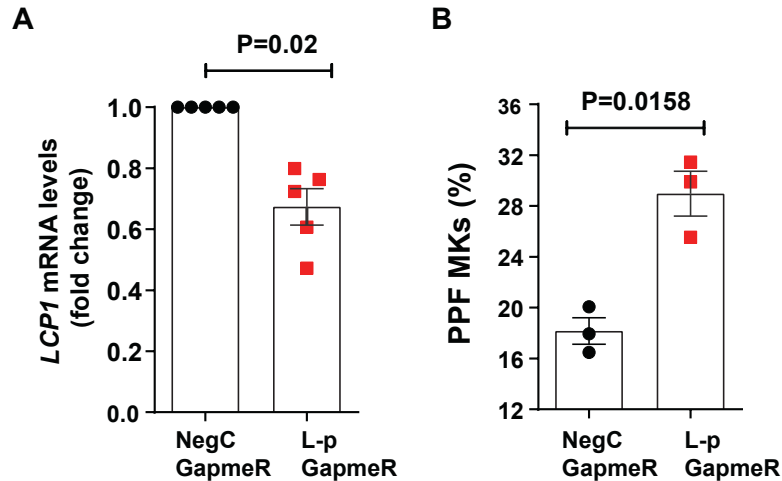
Supplemental Figure 8. *miR-125a-5p* regulates MK L-plastin. Fold changes of densitometric quantification of L-plastin immunoblots after *miR-125a-5p* vs. conL overexpression, normalized to actin (n=8).

A**B**

	IgG	Ago
<i>miR-125a-5p</i>	29.04	23.32
<i>LCP1</i>	40	33.72
<i>U6</i>	24.24	24.88

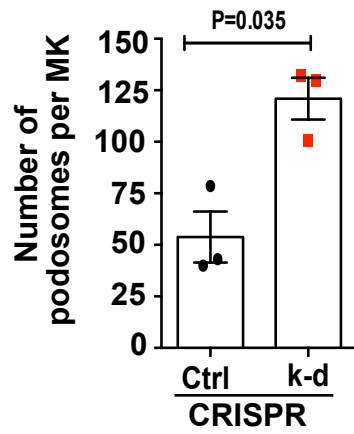
Supplemental Figure 9. *miR-125a-5p* and *LCP1* RNAs enriched in argonaute precipitates.

A. Ethidium stained gel of real time PCR products. CD61+ MKs were isolated, lysed immunoprecipitated with irrelevant IgG or A8 antibody specific for argonaute 2 (Ago2), total RNA extracted, and real time PCR performed using primers specific for *miR-125a-5p* and *LCP1*. There was no enrichment by Ago2 immunoprecipitation of *U6*, a negative control RNA not predicted to be a *miR-125a-5p* target by miRwalk 2.0 software (data not shown). **B.** Table shows Ct values from qPCR for *miR-125a-5p*, *LCP1* and *U6* on Ago enrichment, compared to IgG control (n=1).



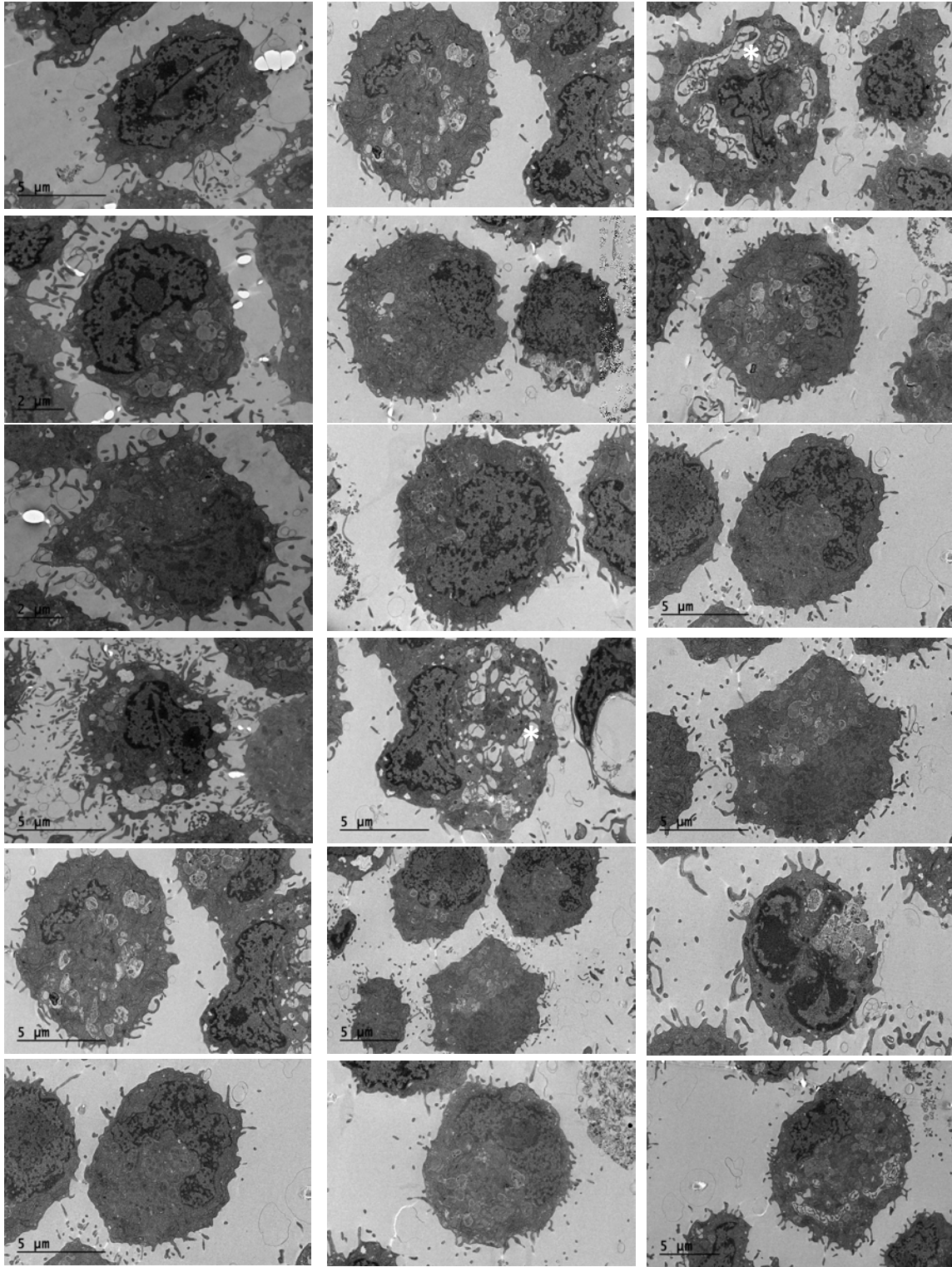
Supplemental Figure 10. *LCP1* inhibition by LNA GapmeR increases MK PPF. **A.** LNA GapmeR against negative control (negC) or *LCP1* (L-p) GapmeR was added at 500 nM on days 3, 6 and 9. Day 13 cultured MKs were harvested for RNA and *LCP1* mRNA levels were determined. Fold changes of *LCP1* levels was plotted for negC vs. L-p GapmeR. *ACTB* was used as a normalizer (n=5). **B.** MK PPF on *LCP1* GapmeR inhibition, scored blinded and compared to negC GapmeR (n=3).

Note that the modest decrease in L-plastin mRNA levels led to an increase in PPF that is comparable to the increase observed in CRISPR-mediated ablation of L-plastin shown in Fig 6. This may reflect the fact that *LCP1* levels are low in mature MKs, it did not take a large fold-change to increase PPF. It is also possible or likely that the GapmeRs do not efficiently induce mRNA destruction, but also inhibit translation into L-plastin with the ultimate effect of increasing PPF.

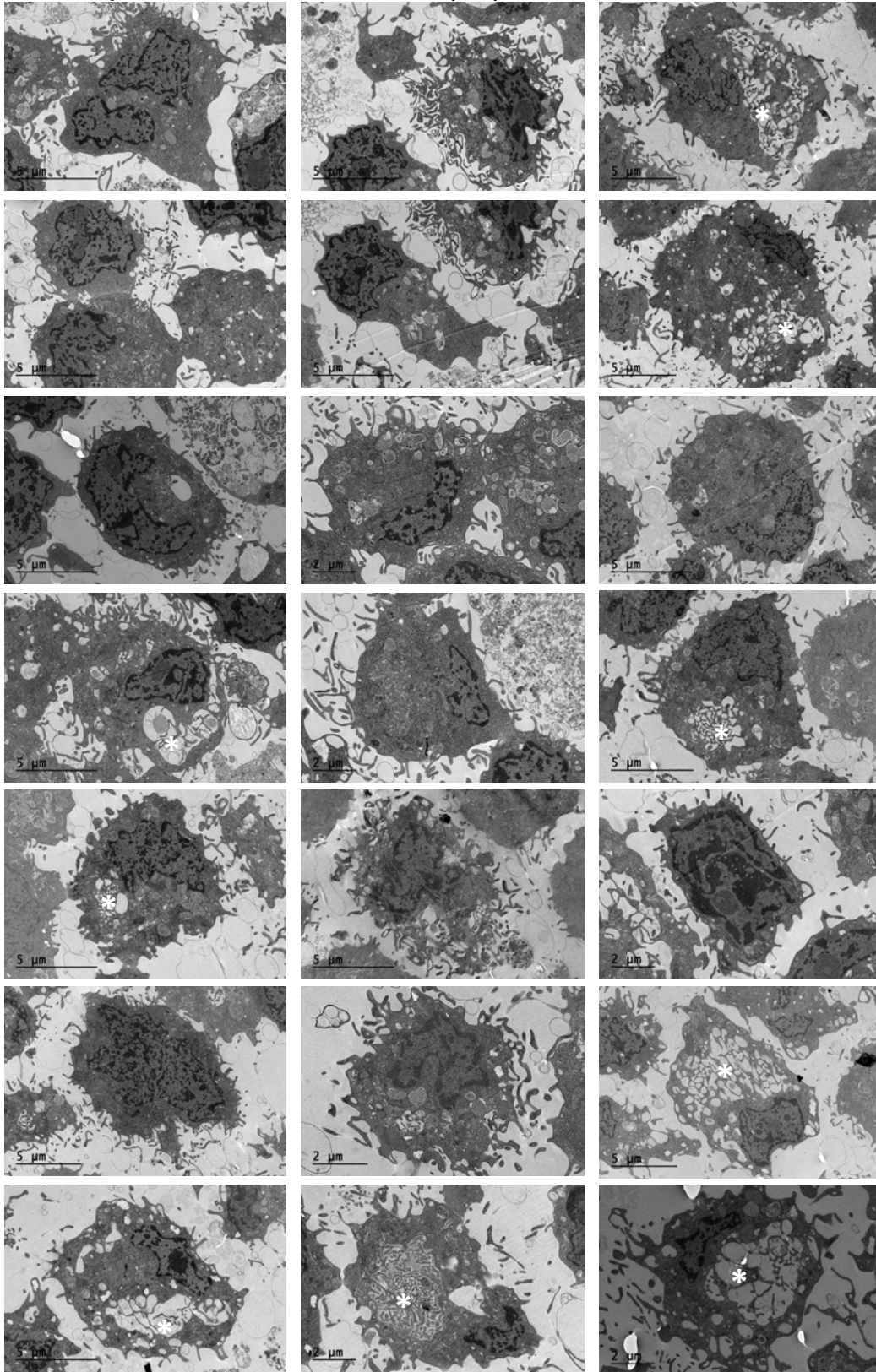


Supplemental Figure 11. The number of podosomes were increased on L-plastin knockdown. Quantification of MK podosomes per MK without or with L-plastin knock-down on day 14 by TIRF (P value from n=3 independent cord blood experiments, at least 10 MKs per condition per cord were analyzed).

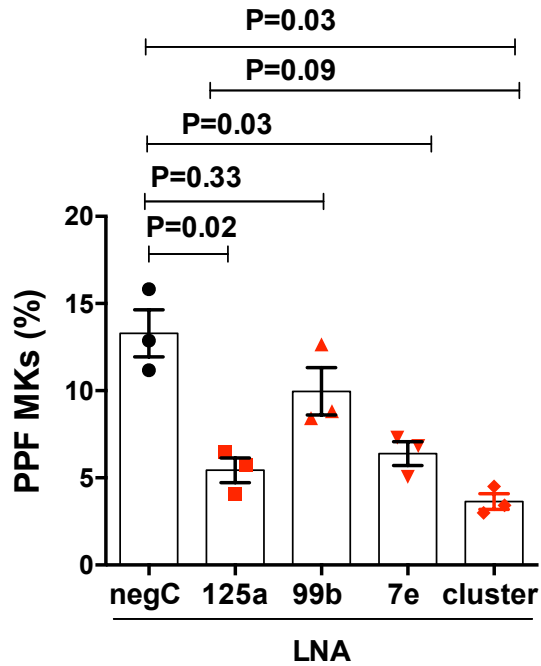
A. Scrambled (scr) control guide RNA CRISPR MKs



B. L-plastin CRISPR knock-down (k-d) MKs



Supplemental Figure 12. Transmission electron microscope images of MKs on L-plastin knock-down. Day 13 MKs treated with non-targeting negative control (ctrl) (panel a) or L-plastin knock-down (k-d) (panel b) CRISPR guide RNA were pelleted, fixed and imaged by TEM. Ctrl (panel A) o k-d (panel b) MKs from three independent cultures are presented. Multiple examples of MKs for each condition are shown. Although there is variation under each condition, L-p k-d (panel b) show more MKs with highly developed IMS than ctrl (panel a) (shown by white asterisk).



Supplemental figure 13: Quantification of proplatelet forming MKs in cultures after *miR-99b/let-7e/miR-125a* cluster inhibition. LNA against negative scrambled control (negC LNA) or *miR-125a-5p* (25a LNA) or *miR-99b-5p* (99b LNA) or *let-7e-5p* (7e LNA) or all three added simultaneously (Cluster LNA) in MK cultures at days 3, 6 and 9. Proplatelet forming (PPF) MKs were counted (blinded as to the treatment group) on day 13 (n=3 independent cultures).

References

1. Edelstein LC, Simon LM, Montoya RT, et al. Racial differences in human platelet PAR4 reactivity reflect expression of PCTP and miR-376c. *Nat Med*. 2013;19(12):1609-1616.
2. Simon LM, Edelstein LC, Nagalla S, et al. Human platelet microRNA-mRNA networks associated with age and gender revealed by integrated plateletomics. *Blood*. 2014;123(16):e37-45.
3. Espina V, Wulfkuhle JD, Calvert VS, et al. Laser-capture microdissection. *Nat Protoc*. 2006;1(2):586-603.
4. Middleton EA, Rowley JW, Campbell RA, et al. Sepsis alters the transcriptional and translational landscape of human and murine platelets. *Blood*. 2019;134(12):911-923.
5. Bhatlekar S, Basak I, Edelstein LC, et al. Anti-apoptotic BCL2L2 increases megakaryocyte proplatelet formation in cultures of human cord blood. *Haematologica*. 2019;104(10):2075-2083.
6. Basak I, Bhatlekar S, Manne BK, et al. miR-15a-5p regulates expression of multiple proteins in the megakaryocyte GPVI signaling pathway. *J Thromb Haemost*. 2019;17(3):511-524.
7. Shi DS, Smith MC, Campbell RA, et al. Proteasome function is required for platelet production. *J Clin Invest*. 2014;124(9):3757-3766.
8. Kawamoto T. Use of a new adhesive film for the preparation of multi-purpose fresh-frozen sections from hard tissues, whole-animals, insects and plants. *Arch Histol Cytol*. 2003;66(2):123-143.
9. Pleines I, Hagedorn I, Gupta S, et al. Megakaryocyte-specific RhoA deficiency causes macrothrombocytopenia and defective platelet activation in hemostasis and thrombosis. *Blood*. 2012;119(4):1054-1063.
10. Xing Z, Lin A, Li C, et al. lncRNA directs cooperative epigenetic regulation downstream of chemokine signals. *Cell*. 2014;159(5):1110-1125.
11. Hamada T, Mohle R, Hesselgesser J, et al. Transendothelial migration of megakaryocytes in response to stromal cell-derived factor 1 (SDF-1) enhances platelet formation. *J Exp Med*. 1998;188(3):539-548.
12. Dunkman AA, Buckley MR, Mienaltowski MJ, et al. The injury response of aged tendons in the absence of biglycan and decorin. *Matrix Biology*. 2014;35:232-238.
13. Teruel-Montoya R, Kong X, Abraham S, et al. MicroRNA expression differences in human hematopoietic cell lineages enable regulated transgene expression. *PLoS One*. 2014;9(7):e102259.
14. Poulter NS, Pollitt AY, Davies A, et al. Platelet actin nodules are podosome-like structures dependent on Wiskott-Aldrich syndrome protein and ARP2/3 complex. *Nature Communications*. 2015;6.
15. Schindelin J, Arganda-Carreras I, Frise E, et al. Fiji: an open-source platform for biological-image analysis. *Nature Methods*. 2012;9(7):676-682.
16. Schneider CA, Rasband WS, Eliceiri KW. NIH Image to ImageJ: 25 years of image analysis. *Nature Methods*. 2012;9(7):671-675.
17. Dweep H, Gretz N. miRWalk2.0: a comprehensive atlas of microRNA-target interactions. *Nature Methods*. 2015;12(8):697-697.

18. Dweep H, Sticht C, Pandey P, Gretz N. miRWalk - Database: Prediction of possible miRNA binding sites by "walking" the genes of three genomes. *Journal of Biomedical Informatics*. 2011;44(5):839-847.